

SELF CALIBRATION OF SMALL AND MEDIUM FORMAT DIGITAL CAMERAS

Donald Moe^a, Aparajithan Sampath^a, Jon Christopherson^a, Mike Benson^b

^aSGT, Inc¹, U.S. Geological Survey (USGS) Earth Resources Observation and Science (EROS) Center, Sioux Falls, SD 57198 USA –(dmoe, asampath, jonchris)@usgs.gov

^bU.S. Geological Survey (USGS) Earth Resources Observation and Science (EROS) Center, Sioux Falls, SD 57198 USA – benson@usgs.gov

KEY WORDS: Photogrammetry, Rectification, Bundle, Camera, Geometric.

ABSTRACT:

The knowledge of a camera’s interior orientation parameters are a prerequisite for the camera to be used in any precision photogrammetric project. Historically, the interior orientation parameters have been determined by analyzing the measured ground 3D coordinates of photo-identifiable targets, and their 2D (image) coordinates from multiple images of these targets. Camera self calibration, on the other hand, uses targets on a scene that have not been measured before. In this research, we will briefly discuss existing self calibration techniques, and present two methods for camera self calibration that are being used at the U.S. Geological Survey’s Earth Resources Observation and Science (EROS) Data Center. The first method, developed by Pictometry (augmented by Dr C.S. Fraser), uses a series of coded targets on a cage. The coded targets form different patterns that are imaged from nine different locations with differing camera orientations. A free network solution using collinearity equations is used to determine the calibration parameters. The coded targets are placed on the cage in three different planes, which allows for a robust calibration procedure. The USGS/EROS has developed an inexpensive method for calibration, particularly for calibrating short focal length cameras. In this case, the coded targets are pasted on a small prototype box and imaged from different locations and camera orientations. The design of the box is discussed, and the results of the box and the cage calibrations are compared and analyzed.

1. INTRODUCTION

1.1 General

Camera calibration procedure aims to completely characterize the path of a ray of light that enters a camera, at the time of exposure. The parameters that are used for this characterization are termed the interior orientation parameters. The main parameters are the focal length of the lens and the location of the principal point of symmetry. However, for photogrammetric purposes, the knowledge of the deviation of the light ray from a straight line, described by polynomial coefficients, is also important. This deviation is termed lens distortion, and the polynomial coefficients are termed lens distortion parameters. The United States Geological Survey (USGS) has the responsibility for camera calibration in the United States (Lee, 2004). In this research, we shall present two methods used by the USGS to determine these parameters for small and medium format digital cameras. The first method, developed by Pictometry(augmented by Dr C.S. Fraser), uses a series of coded targets on a cage. The coded targets are placed on the cage in three different planes, which allows for a robust calibration procedure. The second method describes the development of a method whereby the coded targets are pasted on a small prototype box. The importance of calibrating a camera used for photogrammetric purposes cannot be overstated. While it is possible to obtain accurate ortho-products without a well calibrated camera, these would require a very dense network of control points. Such a network will make a photogrammetric project prohibitively expensive.

| Symbol | Description |
|-----------------|--|
| f | Gaussian focal length |
| K_1, K_2, K_3 | Parameters for radial distortion |
| P_1, P_2 | Parameters for decentering distortion |
| B_1, B_2 | Differential scale distortion (for digital cameras) |
| x_p, y_p | Position of the principal point of symmetry with respect to the array pixel frame. |

Table 1. List of interior orientation parameters

1.2 Camera calibration methods

There are many approaches to camera calibration. With the increasing popularity of the field of Computer Vision as an area of research, the methods have increased. Camera calibration methods preferred by photogrammetrists can be categorized broadly into three classes.

¹Work performed under U.S. Geological Survey contract 08HQCN0005

1.2.1 In-situ calibration: The in-situ methods of calibration are purported to produce the best camera calibration results. They are mostly used for calibrating large cameras that cannot be easily calibrated in laboratories. The cameras are hence calibrated while they are in operation. In-situ calibration methods require an area (a calibration range) with a very dense distribution of highly accurate control points. While maintaining a high density, the control points in the calibration range should be well distributed in the horizontal, as well as in the vertical direction. A rigorous least squares block adjustment based on the co-linearity equations, augmented by equations modelling radial and decentering distortion (Eq. 5) can generate accurate calibration parameters. The in-situ method requires aerial imagery over a calibration range. Also, careful maintenance of the calibration range is required, over the years. The maintenance may include re-survey of the control points, making sure they are undisturbed etc. All these factors can be expensive and time consuming for the camera operators.

1.2.2 Precision multi-collimator instruments: The USGS operates a multi-collimator calibration instrument located at Reston, Virginia, USA (Light, 1992). The instrument is used to calibrate film based cameras, and while digital cameras are increasingly used, there are a number of photogrammetric companies that still employ film cameras. The aerial camera is placed on top of the collimator bank, aligned and focused at infinity. Images that capture the precision targets located in telescopes lens (of the multi-collimator) are taken. The deviation of the measured image (x,y) coordinates from the known (X,Y) coordinates forms the basis for solving for the calibration parameters (Eq. 5).

1.2.3 Self calibration: Self calibration uses the information present in images taken from an un-calibrated camera to determine its calibration parameters (Fraser, 1997; Fraser 2001; Remondino and Fraser, 2006; Strum, 1998). Methods of self calibration include generating Kruppa equations (Faugeras et al., 1992), enforcing linear constraints on calibration matrix (Hartley, 1994), a method that determines the absolute quadric, which is the image of the cone at a plane at infinity (Triggs). While there are many techniques employed by researchers (Hartley, 1994; Faugeras et al., 1992), most of these do not find solutions for distortion and principal point, as they are not considered critical for Computer Vision. On the other hand, for photogrammetrists, these are critical parameters necessary to produce an accurate product at a reasonable price.

In this study, we will use self calibration techniques to determine camera calibration parameters. Section 2 provides a brief theoretical framework for calibration. It goes on to discuss the design of two methods for self calibration used at the USGS, and describes the experimental set-up. It introduces an inexpensive method for calibrating small and medium format digital cameras, with short focal length. Section 3 analyses the results of calibration, and compares the results obtained from the two methods described in Section 2. Section 4 presents the conclusions and discusses future work.

2. CALIBRATION METHODOLOGY

2.1 Theoretical basis

The self calibration procedure described in this research is based on the least squares solution to the photogrammetric resection problem. The well known projective collinearity equations form the basis for the mathematical model.

$$x - x_p = -f \left[\frac{m_{11}(X - X_c) + m_{12}(Y - Y_c) + m_{13}(Z - Z_c)}{m_{31}(X - X_c) + m_{32}(Y - Y_c) + m_{33}(Z - Z_c)} \right] \quad (1)$$

$$y - y_p = -f \left[\frac{m_{21}(X - X_c) + m_{22}(Y - Y_c) + m_{23}(Z - Z_c)}{m_{31}(X - X_c) + m_{32}(Y - Y_c) + m_{33}(Z - Z_c)} \right]$$

In Eq. 1, (x, y) are the measured image coordinates of a feature and (x_p, y_p) are the location of the principle point of the lens, in the image coordinate system, f refers to the focal length and

$\begin{pmatrix} m_{11} & m_{12} & m_{13} \\ m_{21} & m_{22} & m_{23} \\ m_{31} & m_{32} & m_{33} \end{pmatrix}$ is the camera orientation matrix. Since the lens

in the camera is a complex system consisting of a series of lenses, the path of light is not always rectilinear. The result is that a straight line in object space is not imaged as one in the image. The effect is termed distortion. Primarily, we are interested in characterizing the radial distortion and de-centering distortion. Radial distortion displaces the image points along the radial direction from the principal point (Mugnier et al., 2004). The distortion is also symmetric around the principal point. The distortion is defined by a polynomial (Brown, 1966; Light, 1992).

$$\begin{aligned} \delta r &= k_1 r^3 + k_2 r^5 + k_3 r^7 + \dots \\ r &= \sqrt{(x - x_p)^2 + (y - y_p)^2} \end{aligned} \quad (2)$$

$k_i, i = 1, 2, 3, \dots$ are coefficients of the polynomial

The (x,y) components of the radial distortion are given by:

$$\begin{aligned} \delta x_1 &= x \frac{\delta r}{r} \\ \delta y_1 &= y \frac{\delta r}{r} \end{aligned} \quad (3)$$

The second type of distortion is the decentering distortion. This is due to the displacement of the principle point from the centre of the lens system. The distortion has both radial and tangential components, and is asymmetric with respect to the principal point (Mugnier et al., 2004). The components of de-centering distortion, in the $x-y$ direction are given by

$$\begin{aligned} \delta x_2 &= P_1(r^2 + 2x^2) + 2P_2xy \\ \delta y_2 &= 2P_1xy + P_2(r^2 + 2y^2) \end{aligned} \quad (4)$$

A third distortion element, specific to digital cameras accounting for scale distortion of pixel sizes in the x and y direction is also incorporated

$$\delta x_3 = B_1x + B_2y \quad (5)$$

The final mathematical model is a result of adding Eqs. 3 and 4 and 5 to the right hand side of Eq.

$$\begin{aligned} x - x_p &= -f \left[\frac{m_{11}(X - X_c) + m_{12}(Y - Y_c) + m_{13}(Z - Z_c)}{m_{31}(X - X_c) + m_{32}(Y - Y_c) + m_{33}(Z - Z_c)} \right] + \delta x_1 + \delta x_2 + \delta x_3 \\ y - y_p &= -f \left[\frac{m_{21}(X - X_c) + m_{22}(Y - Y_c) + m_{23}(Z - Z_c)}{m_{31}(X - X_c) + m_{32}(Y - Y_c) + m_{33}(Z - Z_c)} \right] + \delta y_1 + \delta y_2 \end{aligned} \quad (6)$$

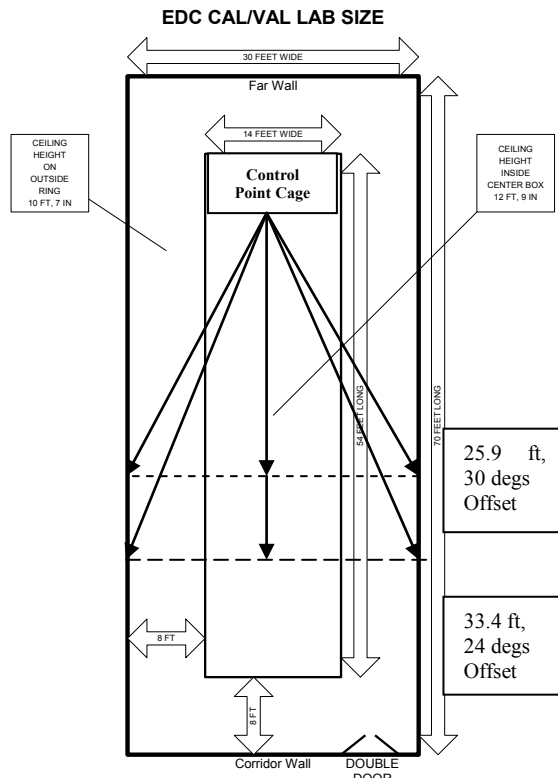
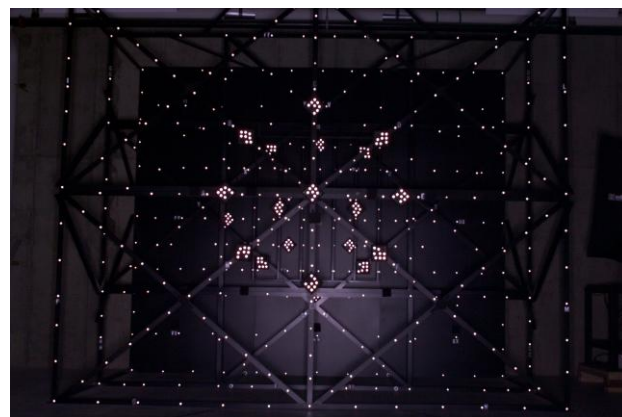


Figure 1. Layout of the calibration lab and the calibration cage

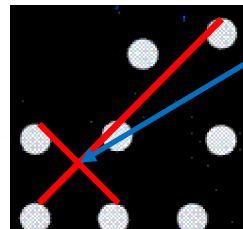
2.2 Experimental set-up for cage based self calibration

The camera calibration facility is located at the USGS’s Earth Resources Observation and Science (EROS) Data Center in Sioux Falls, South Dakota. Fig. 1 shows the position of the calibration cage, with respect to the room. Also shown are some of the positions for locating the cameras. The cage consists of three parallel panels. Each panel has a number of circular retro-reflective targets (dots), and a few coded targets (Fig 2a). The coded targets are so referred because the pattern of the placement of the individual circular dots that make up these targets is unique (Fig. 2b). Each coded target has five dots that are positioned in the same relative orientation as the red lines shown in Fig. 2(b). The intersection of the red lines is taken as the centre of the coded target.

For the calibration procedure, the camera lens is always focussed at infinity. The choice of the distance of the camera from the front panel of the cage depends on the focal length of the camera, and the depth of focus that has been selected. Once the camera-cage distance is fixed, three angular positions from the centre of the front panel of the cage are selected. The angular positions are selected keeping in mind the optimal angles for convergent photography, and the limitations imposed by the dimensions of the calibration room. Ideally, the angular positions will be close to what is shown in Fig 1. Once the images are captured, they are processed using software called Australis (Fraser, 2001). Australis uses a free network method of bundle adjustment. It recognizes the patterns in the coded targets and calculates their centre.



(a) 3D Calibration cage



(b) Coded target



(c) Circular target

Figure 2. (a) Image of the calibration cage, with three panels (b) the pattern in a coded target and (c) the individual circular target

The coded target centre is not the actual centroid of the individual target dots, but determined in a manner shown in Fig. 2(b). The software requires at least four coded targets in each image that are common with other images. It uses the targets to determine the initial relative orientation of the camera at all the exposure stations. It then uses the circular targets to determine a free network least squares bundle adjustment solution of Eq. 5. Since it is a free network solution, the least squares iteration converges easily, and a relative measure of the geometry of the system (the lens, camera, and the targets) is obtained.

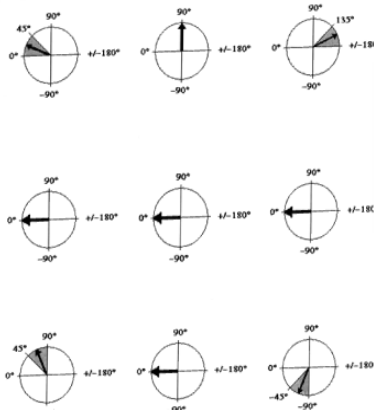


Figure 3. Camera orientations for the nine convergent image exposure stations

2.3 Camera self calibration using a box

With the ever increasing use of digital photography for aerial mapping, the USGS receives many requests to calibrate cameras that are not traditionally used for photogrammetric mapping. Some of these cameras are short focal length small format commercial cameras, (used perhaps from unmanned aerial vehicles, etc.) To handle these requests, the USGS has developed a self calibration procedure that does not require establishing a large calibration cage. Instead, a smaller rigid box that can be easily designed and constructed is used. The current design of the box is as shown in Fig. 4.



Figure 4. A rigid box design for calibration of small format cameras

The box is designed such that its dimensions are approximately 24 inches at the top (outer edge) and 12 inches at the bottom (inner). The inner walls of the box are not vertical, but are sloping at approximately 30 degrees. A scaled down series of coded targets are pasted on all the interior surfaces of the box. The design takes advantage of the simplicity of the free network bundle adjustment solution that requires no outside control structure.

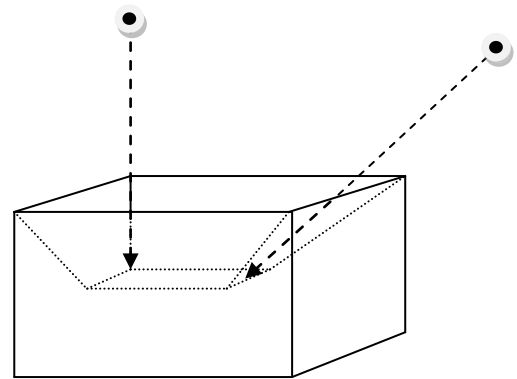


Figure 5. Camera exposure stations for box based calibration

For calibration photography, the optic axis of the camera is usually kept parallel to the inclined interior walls of the box. Three images are obtained from each side, and one image is obtained from each of the four corners, which results in a total of sixteen images. The images are alternatively taken in portrait and landscape modes. For a stable solution, as many targets as possible are obtained from the corners of the camera lens.

3. RESULTS AND ANALYSIS

A Nikon D1x digital single lens reflex (SLR) camera with a 20mm focal length lens (Nikkon AF) was used for this research. F # of 8 was chosen for calibrating with the cage as target, and f # of 22 was chosen for calibrating with the box as the target. The optimal hyperfocal distances for the F# (depth of focus) were calculated using Eq. 6:

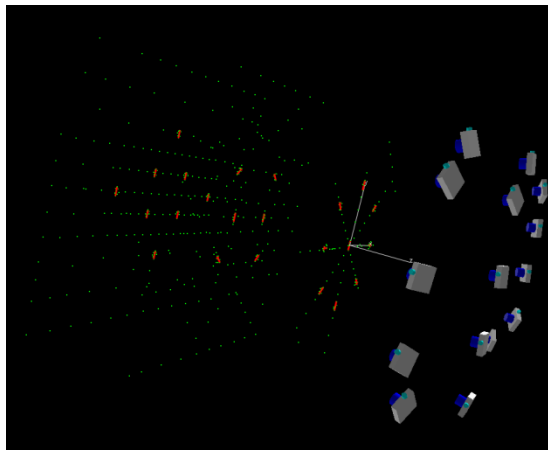
$$H_p = \frac{f^2}{F\# \times c} + f \quad (6)$$

where f is the focal length, and c is the circle of confusion and is approximately 0.072 mm. The hyperfocal distance for the cage was 2.3 ft and for the box was ~ 1ft.

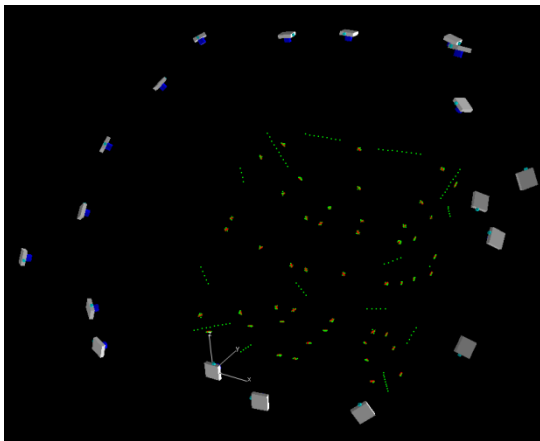
3.1 Results

Since the hyperfocal distance to the front panel of the cage was only 2.4 ft, it was very difficult to cover the entire cage, and the circular and coded targets. To ensure a more complete coverage, it was decided to take more than the standard set of nine images for calibration. A total of 15 images were used in Australis. The free network bundle adjustment solution is graphically displayed in Fig 7 (a). In a similar manner, the hyperfocal distance for the calibration using the box was calculated at 1 ft. A total of 20 images were obtained for the box. The free network solution is graphically shown in Figure 7 (b). The

green dots in Fig. 6 represents a circular target (Fig 2c), while the orange lines represent the coded target patterns (Fig. 2b).



(a)



(b)

Figure 6. Graphical representation of the bundle adjustment solution for (a) Cage and (b) Box based camera calibration

| Calibration parameters | | Calculated values from cage | Calculated values from box |
|-------------------------------------|-------|-----------------------------|----------------------------|
| Focal length | | 20.601 | 20.603 |
| Principle point location | x_p | 0.056 mm | 0.064 mm |
| | y_p | -0.020 mm | -0.019mm |
| Radial distortion coefficients | K1 | 2.781e-004 | 2.74196e-004 |
| | K2 | -4.996e-007 | -4.1747e-007 |
| | K3 | 9.139e-011 | -1.5359e-011 |
| De-centring distortion coefficients | P1 | -6.173e-007 | 2.989e-007 |
| | P2 | 8.341e-006 | 2.637e-005 |
| Scaling elements | B1 | 8.1521e-005 | 1.5082e-005 |
| | B2 | -1.0153e-005 | 9.6088e-006 |

Table 2 Camera calibration parameters

Table 2 shows the solutions to the bundle adjustment and the calibration parameters obtained from the two experiments. Table 2 lists the calibration parameters that were obtained as a part of the bundle adjustment solution

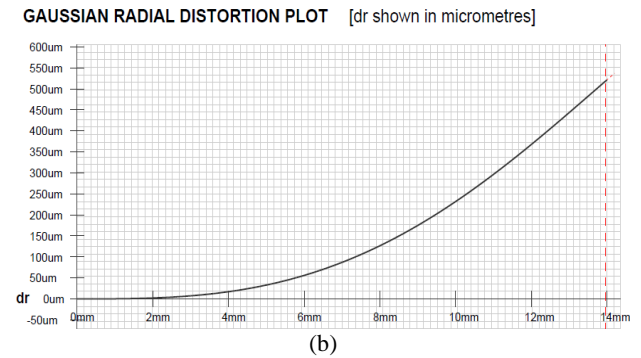
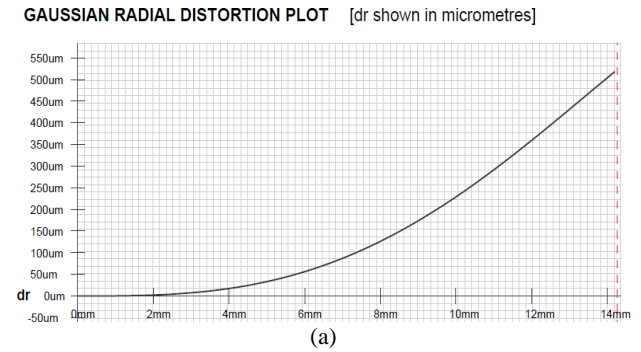


Figure 7. Radial distortion plots showing the distortion (Y-axis, μm) as a function of distance (X-axis, mm) from the principal point for results of camera calibration obtained from (a) Cage and (b) Box. The plots are obtained from Australis software

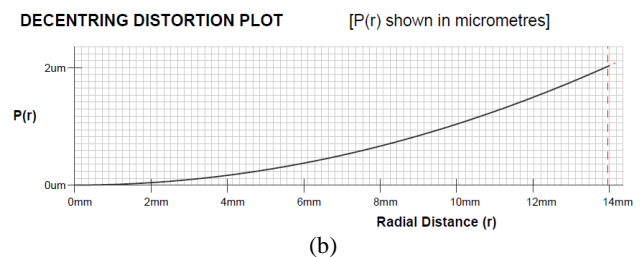
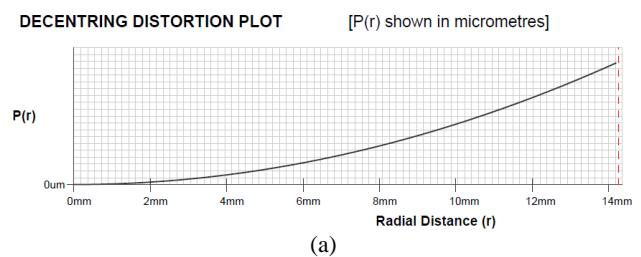


Figure 8. Decentering distortion plots showing distortion (Y-axis, μm), against radial distance (X-axis, mm) for results of camera calibration obtained from (a) Cage and (b) Box. The plots are obtained from Australis software

3.2 Analysis

The results of the two calibration procedures indicate that the parameters are close to being identical (Table 2). The charts in Fig. 7 also show the same phenomena. However, in our experiments, we found that the results start varying if the camera is positioned too close to the targets. This observation seems consistent with previously reported studies on close range photogrammetric camera calibration (Brown, 1971). However, more analysis needs to be done for anything conclusive. Since the Box as a calibration target is meant for small format short focal length cameras, the distance between the targets and the cameras should be close enough so that Australis software is able to recognize the targets. The size of the targets, therefore, needs to be selected accordingly.

4. CONCLUSIONS

In this research, two methods of camera calibration that are used at the USGS EROS at Sioux Falls, South Dakota, USA were presented. The camera calibration lab is housed primarily to calibrate medium format digital cameras, with a focal length range between 20-120mm. The main calibration method uses the principles of self calibration and bundle adjustment on coded targets located on an aluminium cage. A second method to perform calibration was presented. This method used a scaled down version of the coded targets pasted on a small rigid box. Both the methods involve taking images of the targets from different camera locations and orientations. The solution to the bundle adjustment problem is obtained using the software Australis. It was shown that the solutions camera calibration parameters obtained from both the methods are close to each other. The same time the approach using the box yields promising results and can be used for verification of the calibration parameters. Further research on the box by adding more targets may yield results closer to the results obtained from the cage. There has been an increasing interest in calibrating longer focal length cameras (> 150mm) using self calibration methods. The problem becomes non trivial given the limitations of space. Further research is being conducted at the USGS on expanding the range of cameras, with regards to the focal length, that can be calibrated in the lab.

References:

Brown, D.C., 1996. Decentering distortion of lenses. *Photogrammetric Engineering*, 32(3):444– 462.

Brown, D.C., 1996. Close-range camera calibration. *Photogrammetric Engineering*, 37(8):855– 866, August 1971

Faugeras, O., Luong, Q.T. and Maybank, S., 1992. Camera selfcalibration: Theory and experiments. *ECCV'92, Lecture Notes in Computer Science*, Vol. 588, Springer-Verlag, pp. 321-334

Fraser, C.S., 1997. Digital camera self-calibration. *ISPRS Journal of Photogrammetry & Remote Sensing* 52, pp. 149–159, 1997.

Fraser, C.S., 2001. Australis: software for close-range digital photogrammetry users manual.

Hartley, R., 1994: Euclidean reconstruction from uncalibrated

views. In *Applications of Invariance in Computer Vision*, Mundy, Zisserman and Forsyth (eds.), *Lecture Notes in computer Science*, Vol. 825, Springer-Verlag, pp. 237-256

Remondino, F., Fraser, C.S., 2006. Digital camera calibration methods: considerations and comparisons. *IAPRS volume XXXVI, part 5, Dresden 25-27 September 2006*

Lee, G.Y.G. ,2004. Camera calibration program in the United States: past, present and future. In *Post-Launch Calibration of Satellite Sensors*, *ISPRS Book Series*, Vol. 2, A.A. Balkema Publishers, New York.

Light, D.L.,1992. The new camera calibration system at the U.S.Geological Survey. *Photogrammetric Engineering and Remote Sensing*, 58(2):185–188.

Mugnier, C.J., Forstner, W., Wrober, B., Padres, F., Munjy, R., 2004. The mathematics of photogrammetry. In *Manual of Photogrammetry*, Fifth edition. Pp. 181-316.

Strum., P., 1998. A case against Kruppa's equations for camera self-calibration. *IEEE International conference on image processing*, Chicago, Illinois, pp. 172-175.

Triggs, B., 1997. Autocalibration and the absolute quadric, *CVPR*, pages 609–614, Puerto Rico, June 1997.

DISCLAIMER

Any use of trade, product, or firm names is for descriptive purposes only and does not imply endorsement by the U.S. Government.

ACKNOWLEDGEMENTS

Sam Johnson and Alonso Holmes performed most of the camera calibration experiments